ARTÍCULO CIENTÍFICO

STUDY OF THE NOZZLE ANGLE IN A COAXIAL FLOW FOR MILK DROP FORMATION

*María José Ramírez-Rivera and Christian O. Díaz-Ovalle**

Abstract

The generation of liquid particles is remarkable in food processes and depends on the nozzle angle. This work theoretically analyzes how the nozzle angle influences an isothermal coaxial flow. This analysis proposed several nozzle angles to determine the behavior of the droplets inside the system. The Computational Fluid Dynamics simulated milk droplets under a fluid-particle interaction. The results demonstrated that the nozzle angle modifies the flow patterns and generates a mixing zone of particles close to the injection point. The lower nozzle angles yield a reduced mixing zone. These results are previous elements for the spray drying process of milk.

Keywords:
CFD, turbulence, particle tracking

Resumen

La formación de partículas líquidas es importante en los procesos de alimentos y depende del ángulo de aspersión. Este trabajo analiza teóricamente el efecto del ángulo de aspersión en un flujo coaxial isotérmico. Varios ángulos de aspersión son propuestos para observar el comportamiento de las partículas dentro del sistema. La herramienta de Dinámica Computacional de Fluidos simuló partículas de leche bajo una interacción fluido-partícula. Los resultados indican que el ángulo de aspersión modifica la trayectoria del flujo y genera una zona de mezclado de partículas cercano al punto de inyección. Los ángulos de menor tamaño lograron una reducida zona de mezcla. Estas observaciones son elementos preliminares para el análisis del secado de aspersión de partículas de leche.

Palabras claves:
CFD, turbulencia, trayectoria de partículas

Departamento de Ingenierías, Tecnológico Nacional de México/I. T. Roque
carretera Celaya-Juventino Rosas km 8.0 Celaya, Gto., 38124, México
*Autor de correspondencia: christian.do@roque.tecnm.mx

1. Introduction

Spray flows are reclaimed in most processes in the food industry. Sirignano (2010) and Ashgriz (2011) have conducted the mathematical formulation of this flow, where a multi-factorial system dominates the spray generation, such as tension forces, liquid properties, pressure, temperature, etc. Nevertheless, Michaelides et al. (2017) have declared a complex nature of the spray flow and proposed a diversity of classes and phenomena during the liquid breakup through a nozzle. Fritsching (2004) has described the main elements of simulating spray flows via Computational Fluid Dynamics (CFD). Besides, the study of spray flows and particle formation from a nozzle is an extended topic, and this study follows brief and selected works to avoid an exhausting review.

The particle injection flow has presented diverse approaches to predict the particle behavior through a coaxial flow. Experimentally, Liu et al. (2012) tested the granular jet mass flux in the wavy fluid flow and the oscillating dispersion regime based on the Strouhal number. Their results presented three-phase interface behaviors in response to the air jet velocity, where the granular jet becomes discontinuous near the nozzle orifice. Fang et al. (2015) found that the gas backflow influences the entrainment phenomena in the particles. They indicated the existence of a critical annular gas velocity for granular streams and the reverse dispersion angle. In detail, Fang et al. (2017) studied granular coaxial jets where a recirculation zone appears when the annular gas velocity increments. This flow yields a negative pressure zone in the surroundings. The injection position remarkably influences the particle recirculation. Similarly, Ba et al. (2022) observed how the nozzle contract angle influences the hydrodynamic behavior of the particles, and the concentration increases near the nozzle exit. And, Ba et al. (2023) studied an annular coaxial nozzle and found the existence of vortices in the particle flow pattern.

Although all these works declared important flow patterns during injections, the theoretical studies have reached remarkable advances in this phenomenon, and the CFD technique models such elements through a jet injection to form a discrete phase in a Eulerian-Eulerian approach (Fritsching, 2004). Pedel et al. (2014) simulated the dispersed particulate phase in their code for LES (Large Eddy Simulation) and found segregation effects in the small particle flowthrough. Patro et al. (2016) developed a mixture model for a Eulerian-Eulerian approach for a co-flow system where a high loading reduces the gas phase velocity. Liu et al. (2023) exposed an LES subgrid-scale model with four-way coupling, and the results presented a swirling flow zone due to the pressure gradients and the internal toroidal recirculation. The swirling inner flow extends to the external flow field and generates a vortex ring of similar size to the jetting nozzle. Zhang et al. (2024) solved a coaxial flow in a supercritical fluid where the particles close to Stokes <1 followed the flow streamlines otherwise the particles were freer in the fluid field.

The nozzle design has been modified to understand the particle flow. Yu et al. (2012) tested different nozzles under several turbulence models, where the ring nozzle increases the turbulence intensity, and the Reynolds Stress Model predicts accurate results for turbulent fluctuations. And, Alam et al. (2016) provided a detailed design of nozzles by varying the configuration in diverse angles and demonstrated the insignificant effect on the shear layer of the nozzle angle.

Due to the lack of experiments for predefined operative parameters of nozzles, e.g., the nozzle angle, cone diameter, etc., the literature has not specified their significance level in the flowthrough. This study describes the effect of the cone angle in a whole conical nozzle during a coaxial flow of milk and advances in particle distribution to prevent particle agglomeration in food processes, such as spray drying.

2. Methodology

This study considers a cylindrical chamber with an inlet airflow interacting with milk drops without evaporation in an isothermal process. The injection system consisted of a solid cone (azimuthal angle of 360°) in the same direction as the airflow. The analysis considers several injection angles after spray formation: 5°, 20°, 40°, 60°, and 80°. The commercial CFD package ANSYS® Fluent 2024 R1 developed the numerical simulations by following the conventional CFD strategy: a) creation of the computation domain, b) meshing of the system, and c) testing of the injection angles.

2.1 Description of the system

The cylindrical chamber is 24 cm in diameter and 1 m in height. The air enters at 27°C by an annular face with 15.5 cm of outer diameter and 8.3 cm of inner diameter (3.6 cm of separation). The injection point is the central upper point of the chamber. Figure 1 a) schematizes the dimensions and parts of the system.

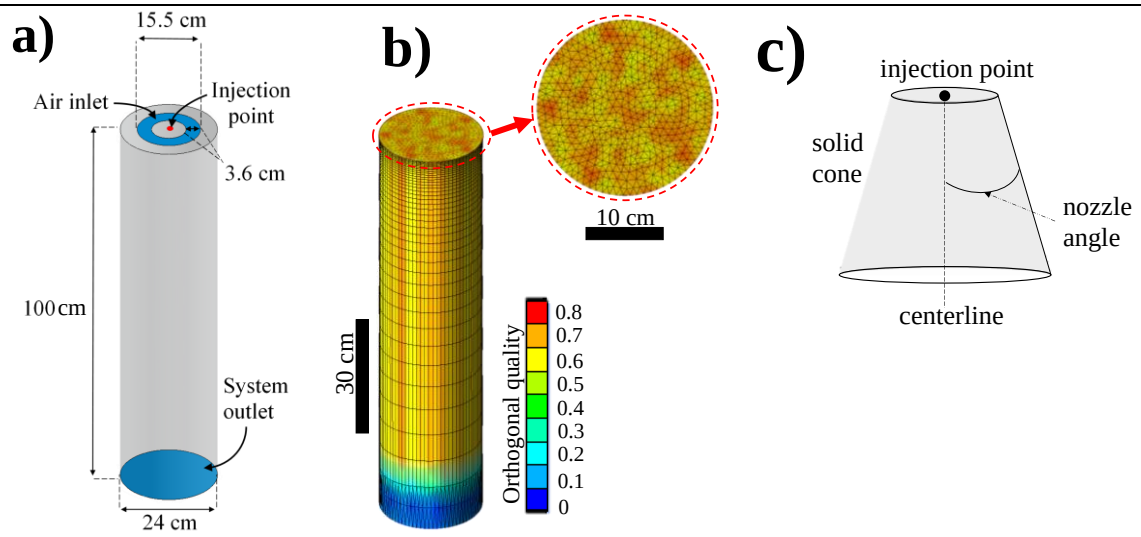

Fig. 1. Cylindrical chamber: a) dimensions and boundary conditions, b) proposed mesh with the orthogonal quality profile, c) nozzle angle definition.

2.2 Meshing of the system

The discretizing process yields control volumes (cells or mesh) into the computational domain. For this case, the cells are 46,177 tetrahedron elements under a growing pattern from the upper section to the lower face, with precision increments during the numerical solution for the formation of milk drops. Nevertheless, the mesh quality is an important indicator to reduce numerical errors during the solution. Herein, diverse parameters measure the mesh quality, where the orthogonal quality is selected. This parameter corresponds to the ratio of the distance of the centroid of the orthogonal vector of the cell and the distance of the centroid of the cell, and the desired values are close to 1 (one). Figure 1 b) depicts the mesh for this study and the orthogonal quality profile.

2.3 Boundary conditions

The airflow is 8.4 m/s at 27°C with a low level of turbulence that equates to turbulence intensity of 5%. The milk drops are 1027 kg/m^3 of density, 0.048 N/m of surface tension, 0.002314 kg/ms of viscosity (Frías-Esquivel et al., 2017), and an average diameter of 20 µm. The size distribution corresponds to 10 different diameters from 1 µm to 30 µm under the Rosin-Rammler distribution. The conical injection is 0.01 kg/s and 0.5 m/s.

2.4 Governing equations

The system is an isothermal flow under a steady state that conserves mass, momentum, and turbulence. Herein, the κ-ε realizable model describes the turbulence and considers the alternative formulation for the turbulence viscosity with a better spectral energy transfer in the turbulent flow and without singularities in the destruction term of turbulence (Yeoh & Yuen, 2010). Table 1 contains the governing equations for this study.

Table 1. Governing equations.

Name	Equation
Mass conservation	$\nabla \cdot \rho \mathbf{v} = 0$
Momentum conservation	$\nabla \cdot \rho \mathbf{v}\mathbf{v} = -\nabla p - \nabla \cdot \boldsymbol{\tau} + \rho \mathbf{g} + \frac{18\mu}{\rho_p d_p^2} \frac{\mathrm{Re} C_D}{24} \left(\mathbf{v} - \mathbf{v}_p \right)$
Kinetic turbulence energy	$\nabla \cdot \rho \kappa \mathbf{v} = \nabla \cdot \left(\mu + \mu_t / \sigma_\kappa \right) \nabla \kappa - \rho \varepsilon$
Dissipation of turbulence	$\nabla \cdot \rho \varepsilon \mathbf{v} = \nabla \cdot \left(\mu + \mu_t / \sigma_\varepsilon \right) \nabla \varepsilon + \rho C_1 S \varepsilon - \rho C_2 \varepsilon^2 / \left(\kappa + \sqrt{\nu \varepsilon} \right)$
Discrete phase	$\frac{d\mathbf{v}_p}{dt} = \frac{18\mu}{\rho_p d_p^2} \frac{\mathrm{Re} C_D}{24} \left(\mathbf{v} - \mathbf{v}_p \right) + \mathbf{g} \left(\frac{\rho_p - \rho}{\rho} \right)$
Notation	$S = \sqrt{2\mathbf{S} : \mathbf{S}}, \quad \text{with} \quad \mathbf{S} = \left(\nabla \mathbf{v} + (\nabla \mathbf{v})^T \right) / 2$

2.5 Numerical solution

The SIMPLE algorithm solved this case study and considered the second-order upwind discretization approach under a hybrid initialization. The calculation demanded around 25 min per simulation to reach 1000 iterations in a steady state. The solution was possible in an Intel® Corel ™ i7-3770 3.4 GHz computer with 24 GB RAM.

3. Results

This study compares diverse nozzle angles during the spread of milk drops to contact the coaxial flow. Figure 1 c) depicts diverse proposed nozzle angles. After spread, all cases presented an evaporation region near the injection point and produced a divergent trajectory of milk drops. This behavior results from the water vapor formation that blocks the drops instead of yielding a whole jet stream.

Figure 2 depicts the velocity profile into streamlines and the particle diameter distribution. The airflow produces a recirculation zone close to the walls at the upper section. Fang et al. (2015) experimentally observed the same phenomenon in granular streams for different gas velocities. The high velocity yields a mixing zone that affects the cone formation in response to the evaporation zone. In the 5° nozzle angle, the milk drops experience a low affectation by the airflow, whereby the flow distributes the milk drops through the system. Thus, the increment of the nozzle angle demonstrates the effect of the airflow that collapses the drop distribution into a mixing zone close to the injection point. The result is a narrow flow through the cylinder.

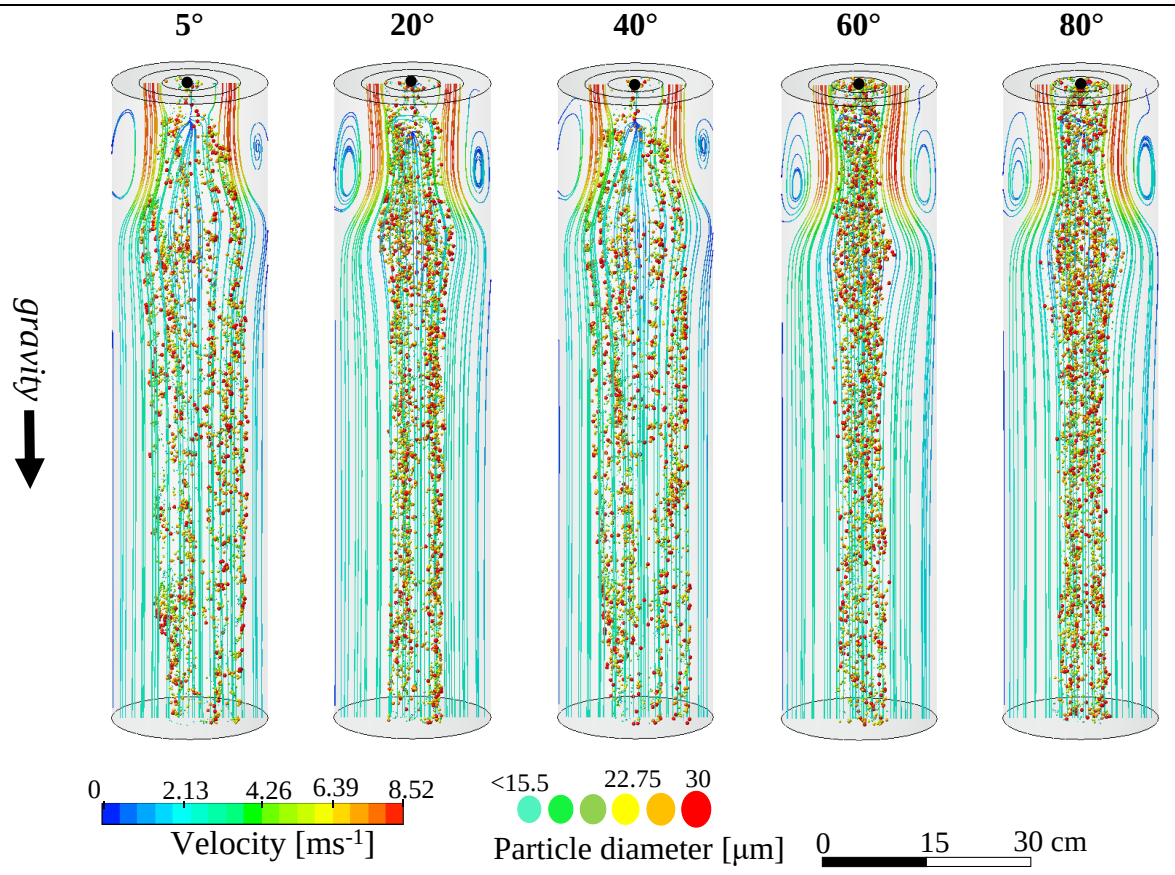

Fig. 2. Streamlines and particle diameters for several nozzle angles: a) 5°, b) 20°, c) 40°, d) 60° and e) 80°.

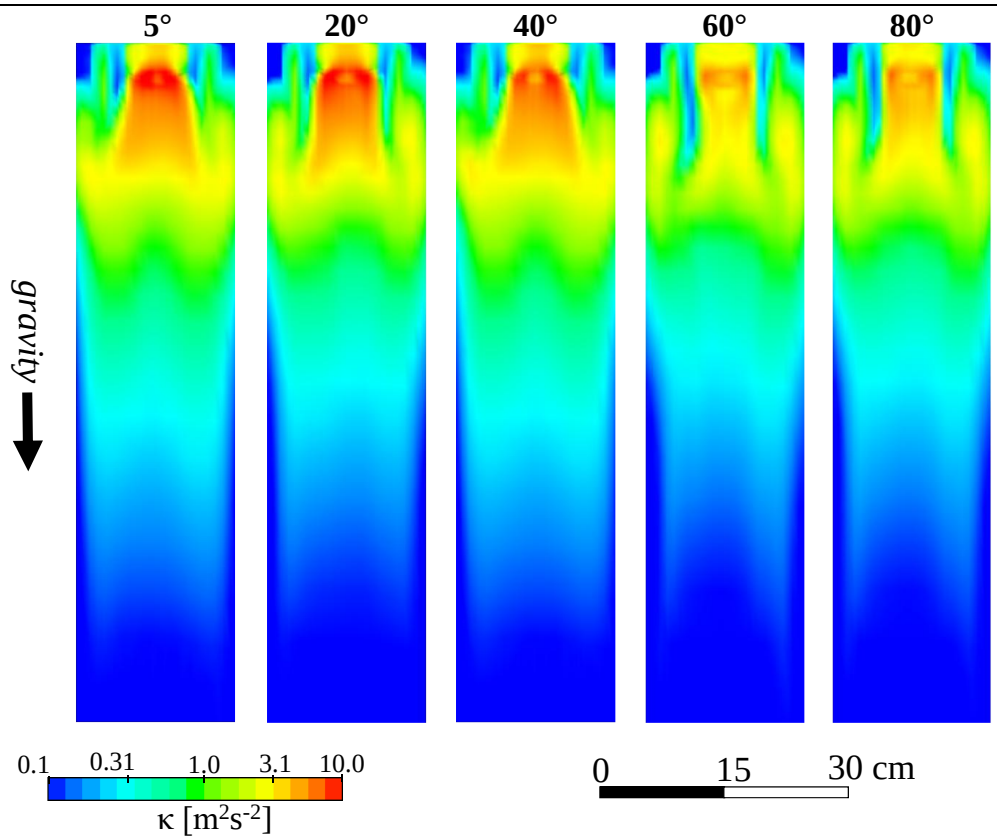

Fig. 3. Profiles of kinetic turbulence energy for several nozzle angles: a) 5°, b) 20°, c) 40°, d) 60°, and e) 80°.

The turbulence kinetic energy explains the level of turbulence for a system. Figure 3 depicts this parameter with an intense turbulence region after the evaporation zone. The nozzle angle influences on the level of turbulence due to the evaporation rate. The narrowness of the case lower angle intensified the turbulence; this response is similar to cases of 20° and 40°. On the other hand, the greater nozzle angles reduce the turbulence level due to the low evaporation rate.

The mass concentration of the milk drops identifies potential evaporation zones, which were not predicted herein. Figure 4 schematizes the distribution of the mass concentration through the cylinder chamber. The cases of 60°, 80°, and 20° presented high mass concentration values, but in particular, the nozzle angle of 60° concentrated the drops in a section where the remaining nozzle angle. In particular, the 40° nozzle angle yields a transitional behavior between the rising of the nozzle angle and the turbulent zone that reduces the particle concentration.

4. Conclusion

The CFD technique has succinctly described the hydrodynamic behavior of the milk drops in a coaxial flow. The results have indicated the remarkable effect of the injection angle on the velocity profile, turbulence intensity, and particle concentration inside the system. The test of several injection angles demonstrated that the low angles do not generate a mixing zone close to the injection point by creating an evaporation zone. These observations contribute to understanding the use of predefined numerical elements to simulate spray injection in CFD tools and extend to simulate food processes, such as spray drying, grain humectation, cleaning systems, etc.

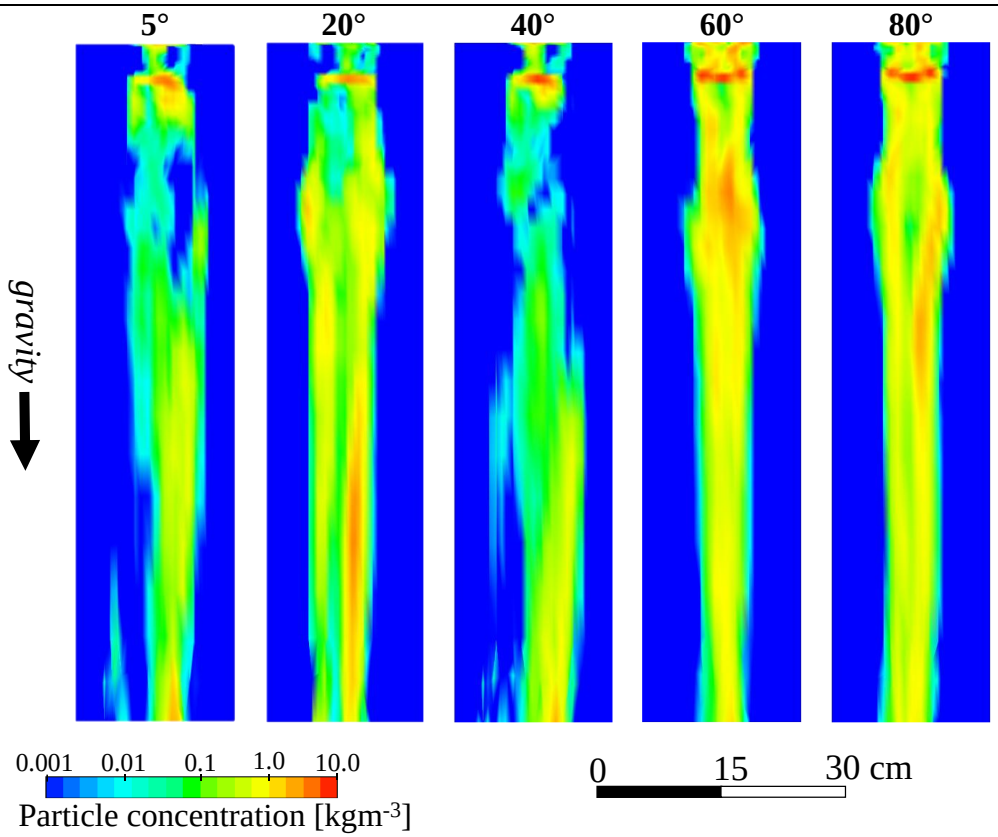

Fig. 4. Profiles of particle concentration for several nozzle angles: a) 5°, b) 20°, c) 40°, d) 60° and e) 80°.

Nomenclature

C_1, C_2	constants of turbulence model
C_D	drag coefficient
d_p	particle diameter
$\mathbf{g}$	vector form of gravity acceleration
p	pressure
Re	Reynolds number
$\mathbf{v}$	fluid velocity vector
$\mathbf{v_p}$	particle velocity vector

Greek letters

ε	rate of dissipation
κ	turbulence kinetic energy
μ	fluid viscosity
μ_t	turbulence viscosity
ρ	fluid density
ρ_p	particle density
σ_κ	turbulent prandtl number for κ
σ_ε	turbulent prandtl number for ε
$\boldsymbol{\tau}$	fluid stress tensor

Acronyms

CFD Computational Fluid Dynamics
SIMPLE Semi-Implicit Method for Pressure Linked Equations

Acknowledgement

The authors appreciate the financial support by CONAHCYT, México through the scholarship 1260180 and SNII.

Declaration

Images used are courtesy of ANSYS, Inc.

References

Alam, M.M.A., Setoguchi, T., Matsuo, S., & Kim, H.D. (2016). Nozzle geometry variations on the discharge coefficient. Propulsion and Power Research, 5(1), 22-33. DOI: 10.1016/j.jppr.2016.01.002.

Ashgriz, N. (Ed.). (2011). Handbook of atomization and sprays: theory and applications: Springer Science.

Ba, Z., Wang, Y., Zhao, J., Hao, Z., Li, C., et al. (2023). Comparative study on gas-particle transport characteristics subjected to the central and annular coaxial jets. Powder Technology, 413, 118080.
DOI: 10.1016/j.powtec.2022.118080.

Ba, Z., Zhao, J., Hao, Z., Li, J., Yang, X., et al. (2022). Effects of the nozzle contraction angle on particle flow behaviors in a gas-particle two-phase jet. Experimental Thermal and Fluid Science, 135, 110624.
DOI: 10.1016/j.expthermflusci.2022.110624.

Fang, C., Xu, J., Zhao, H., Li, W., & Liu, H. (2015). Experimental investigation on particle entrainment behaviors near a nozzle in gas–particle coaxial jets. Powder Technology, 286, 55-63.
DOI: 10.1016/j.powtec.2015.07.041.

Fang, C.C., Xu, J.L., Zhao, H., Li, W.F., & Liu, H.F. (2017). Particle movements in near field induced by thick-wall effect in a dense gas-solid coaxial jet. Powder Technology, 320, 7-13.
DOI: 10.1016/j.powtec.2017.07.018.

Frías-Esquivel, J., González-Alatorre, G., Díaz-Ovalle, C.O., Lesso-Arroyo, R., & Ramos-Ojeda, E. (2017). Hydrodynamic analysis of the falling-film formation in evaporators using CFD simulation. Food and Bioproducts Processing, 101, 56-67.
DOI: 10.1016/j.fbp.2016.10.006.

Fritsching, U. (2004). Spray simulation: modelling and numerical simulation of sprayforming metals: Cambridge University Press.

Liu, H., Cao, W., Xu, J., Li, W., & Sun, Z. (2012). Dispersion mode of granular jet in a coaxial air jet. Powder Technology, 217, 566-573.
DOI: 10.1016/j.powtec.2011.11.022.

Liu, Y., Liu, J., Li, S., Li, G., & Zhou, L. (2023). Hydrodynamic modeling of coaxial confined particle-laden turbulent flow. Energy, 281, 128144.
DOI: 10.1016/j.energy.2023.128144.

Michaelides, E.E., Crowe, C.T., & Schwarzkopf, J.D. (Eds.). (2017). Multiphase flow handbook: CRC Press.

Patro, P., Barik, A.K., & Patro, B. (2016). Computational study of a turbulent gas-solid confined jet flow. Powder Technology, 297, 229-238.
DOI: 10.1016/j.powtec.2016.04.029.

Pedel, J., Thornock, J. N., Smith, S. T., & Smith, P. J. (2014). Large eddy simulation of polydisperse particles in turbulent coaxial jets using the direct quadrature method of moments. International Journal of Multiphase Flow, 63, 23-38.
DOI: 10.1016/j.ijmultiphaseflow.2014.03.002.

Sirignano, W. (2010). Fluid dynamics and transport of droplets and sprays. New York: Cambridge University Press.

Yeoh, G.-H., & Yuen, K.-K. (2010). Computational Fluid Dynamics in fire engineering: Butterworth-Heinemann.

Yu, Y., Shademan, M., Barron, R.M., & Balachandar, R. (2012). CFD Study of Effects of Geometry Variations on Flow in a Nozzle. Engineering Applications of Computational Fluid Mechanics, 6(3), 412-425.
DOI: 10.1080/19942060.2012.11015432.

Zhang, C., Shang, Y., Su, H., Ge, Z., & Guo, L. (2024). Numerical simulation of fluid-particle flow of jet in supercritical water environment. International Communications in Heat and Mass Transfer, 154, 107445.
DOI: 10.1016/j.icheatmasstransfer.2024.107445.